NASA TECHNICAL MEMORANDUM

NASA TM X-2534

NASA TM X-2534

NEUTRONICS ANALYSIS OF AN OPEN-CYCLE HIGH-IMPULSE GAS-CORE REACTOR CONCEPT

by Charles L. Whitmarsh, Jr.

Lewis Research Center

Cleveland, Ohio 44135

NATIONAL AERONAUTICS AND SPACE ADMINISTRATION • WASHINGTON, D. C. • APRIL 1972

1. Report No.	2. Government Accession No.	3. Recipient's Catalog No.
NASA TM X-2534		

4. Title and Subtitle	5. Report Date
NEUTRONICS ANALYSIS OF AN OPEN-CYCLE HIGH-IMPULSE GAS-CORE REACTOR CONCEPT	April 1972
	6. Performing Organization Code
7. Author(s)	8. Performing Organization Report No.
Charles L. Whitmarsh, Jr.	E-6390
	10. Work Unit No.
9. Performing Organization Name and Address	112-28
Lewis Research Center National Aeronautics and Space Administration Cleveland, Ohio 44135	11. Contract or Grant No.
	13. Type of Report and Period Covered
12. Sponsoring Agency Name and Address	Technical Memorandum
National Aeronautics and Space Administration Washington, D.C. 20546	14. Sponsoring Agency Code

15. Supplementary Notes

16. Abstract

A procedure was developed to calculate the critical fuel mass, including the effects of propellant pressure, for coaxial-flow gas-core reactors operating at 196 600 newtons thrust and 4400 seconds specific impulse. Data were generated for a range of cavity diameter, reflector-moderator thickness, and quantity of structural material. Also presented are such core characteristics as upper limits on cavity pressure, spectral hardening in very-high-temperature hydrogen, and reactivity coefficients.

17. Key Words (Suggested by Author(s))	18. Distribution Statement
Nuclear rocket Gaseous reactor Thermal nuclear reactors High-temperature nuclear reactor	Unclassified - unlimited

19. Security Classif. (of this report)	20. Security Classif. (of this page)	21. No. of Pages	22. Price*
Unclassified	Unclassified	36	$3.00

* For sale by the National Technical Information Service, Springfield, Virginia 22151

CONTENTS

NEUTRONICS ANALYSIS OF AN OPEN-CYCLE HIGH-IMPULSE GAS-CORE REACTOR CONCEPT

by Charles L. Whitmarsh, Jr.

Lewis Research Center

SUMMARY

In order to develop a procedure for calculating the critical fuel mass as a function of the propellant pressure, an analytical study was performed on a 196 600-newton-(44 200-lbf) thrust, 4400-second-specific-impulse open-cycle gas-core rocket reactor. Neutron transport calculations were made on a range of reactor configurations so that the required fuel mass and propellant pressure of a given reactor configuration could be calculated for various combinations of cavity diameter, reflector-moderator thickness, and amount of structural material included in the beryllium oxide (BeO) reflector-moderator. The ranges of variables calculated were 3.048 to 4.267 meters (10 to 14 ft) for cavity diameter, 0.457 to 0.762 meter (1.5 to 2.5 ft) for reflector-moderator thickness, and up to 6-volume-percent separated molybdenum as a structural material in the reflector-moderator. The reactor model was a spherical cavity region consisting of a ball of plasma uranium-235 fuel suspended in a hydrogen propellant. The cavity was surrounded by a spherical shell regions of BeO cavity liner, feed hydrogen, BeO reflector-moderator, plenums for helium coolant, and a titanium pressure vessel.

High-temperature (4160 to 22 400 K) hydrogen was observed to significantly affect the neutronics of this reactor. Negative reactivity worths of the order of 15 percent $\Delta k/k$ were attributed to upscattering of neutrons by high-energy hydrogen atoms. Consequently, median fission energies in the range of 0.3 to 0.7 electron volt resulted from hardening of the spectrum of neutrons returning from the reflector to the core region.

In order to increase the mass of uranium fuel contained in this reactor without increasing the uranium loss rate, it is necessary to operate at a high cavity pressure. The net reactivity effect (positive fuel and negative propellant) decreases with increased fuel loading. A limiting pressure was calculated which represents the pressure corresponding to the fuel loading at which this net reactivity effect becomes negative.

Reactivity coefficients were calculated for use in analyses of the dynamic behavior of open-cycle gas-core reactors.

INTRODUCTION

The gas-core reactor concept is applicable to manned interplanetary travel because of its potential for high thrust-to-weight ratio and high specific impulse (refs. 1 to 3). Of interest in this analysis is the open-cycle coaxial-flow concept, in which a critical mass of plasma nuclear fuel is suspended in a reactor vessel by fluid dynamic forces of a hydrogen propellant gas flowing around it. This core is surrounded by a reflector-moderator to reduce fuel requirements. A schematic in figure 1 illustrates the reactor concept as used in this report.

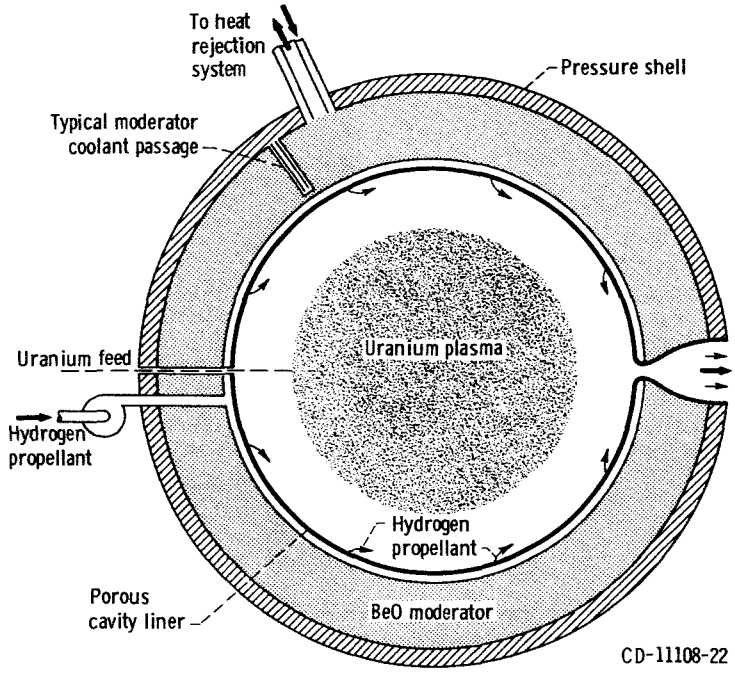

Figure 1. - Schematic of open-cycle gas-core reactor.

Although lower specific impulse (1500 to 2500 sec) concepts have been examined both analytically and experimentally for several years in the coaxial-flow gas-core reactor program at the Lewis Research Center, the concept of high-impulse engines (of the order of 3000 sec or higher) and the design changes required for them are relatively new. One major variation is the use of a high-temperature reflector material and a reflector cooling mechanism (ref. 4) to remove the approximately 7 percent of reactor power that is deposited through neutron and gamma ray absorption. At specific impulses less than 3000 seconds, regenerative cooling was sufficient to remove the neutron and gamma ray heating. To further explore the feasibility of high-impulse gas-core rocket engines, a

design study was initiated to determine the major problem areas and to better define technical feasibility. This report presents the neutronic data generated during that study (ref. 5).

Previous analyses by Hyland (ref. 6) and Ragsdale (ref. 7) indicated the importance of the dependent relation between fuel mass and hydrogen propellant pressure in establishing nuclear criticality and fuel containment in a gas-core reactor. A procedure was therefore developed for calculating a fuel mass which would consider both of these constraints. Thus the calculated fuel mass would provide nuclear criticality and be surrounded by a hydrogen propellant at a pressure sufficient to contain that fuel mass. The procedure would be useful as an engineering design tool since it would allow calculation of the critical mass - reactor configuration - propellant pressure relation for a given set of operating conditions. This feature has been lacking in previous gas-core analyses.

Reported herein are the data from neutron transport calculations which were performed on a range of reactor configurations in order to develop this procedure for various combinations of cavity diameter, reflector thickness, and amount of structural material. Also included are ancillary data obtained in this study which pertain to neutronics effects of high-temperature hydrogen and to reactivity coefficients useful in kinetics analysis.

Ground rules established to facilitate the reactor calculations are as follows:

(1) A thrust of 196 600 newtons (44 200 lbf) and a specific impulse of 4400 seconds were selected based on a mission analysis of a manned Mars trip.

(2) A ratio of fuel diameter to cavity diameter of 0.67 was selected based on experimental cold-flow tests of stagnant gas containment within a flowing gas (refs. 8 and 9).

(3) Uranium enriched in uranium-235 (U^{235}) was used for fuel because of its availability, since usage might exceed 10 000 kilograms per trip (ref. 4). An enrichmant of 98 percent was based on the maximum available in the Atomic Energy Commission separation work cost schedule (ref. 10).

CALCULATIONAL MODEL AND PROCEDURE

Configuration

The basic components of fuel, propellant, reflector, and pressure shell were arranged in a spherical model in such a way as to minimize critical mass while still providing the required functions of fuel containment, cavity liner heat protection, and structural heat removal. The design bases for this reactor configuration and its components are described in reference 5. The analytical model for the neutronics analysis is described in table I. The reactor cavity consists of a core region of plasma fuel, surrounded by propellant hydrogen containing a seed material U^{238}, and bounded by a porous

TABLE I. - DIMENSIONS AND MATERIAL COMPOSITIONS OF SPHERICAL MODEL USED IN CRITICALITY CALCULATION

Region	Average temperature, K	Region thickness, cm	Material[a]	Composition, atm/cm^3
Fuel	50 000	[b]102 [c]122.5 [d]143.1	98 U^{235} 2 U^{238}	Variable fuel loading
Cavity hydrogen (propellant)	10 600	[b]50.4 [c]60.3 [d]70.2	95 wt % H 5 wt % U^{238}	$N^H = 0.290\times10^{21}$ $N^{U^{238}} = 0.614\times10^{17}$
Cavity liner	1 600	1.27	84.7 BeO [b]10 H	$N^{Be} = N^O = {}^e0.0614\times10^{24}$ $N^H = 0.377\times10^{21}$ $N^{U^{238}} = 0.8\times10^{14}$
Feed hydrogen	1 600	1.27	95 wt % H 5 wt % U^{238}	$N^H = 0.00377\times10^{24}$ $N^{U^{238}} = 0.8\times10^{18}$
Reflector edge	------	2.54	94 BeO	$N^{Be} = N^O = 0.0682\times10^{24}$
Reflector[f]	1 600	[g]43.18 [h]58.42 [i]73.66	84.2 BeO 10.5 He	$N^{Be} = N^O = 0.0635\times10^{24}$ $N^{He} = 0.147\times10^{21}$
Hot plenum (coolant outlet)	1 390	1.27	4.7 BeO 95 He	$N^{Be} = N^O = {}^e0.0034\times10^{24}$ $N^{He} = 0.00199\times10^{24}$
Plenum divider	------	1.27	94 BeO	$N^{Be} = N^O = 0.0682\times10^{24}$
Cold plenum (coolant inlet)	1 280	1.27	He	$N^{He} = 0.00228\times10^{24}$
Outer plenum wall	------	1.27	94 BeO	$N^{Be} = N^O = 0.0682\times10^{24}$
Insulation	800	15.24	10 ZrO_2	$N^{Zr} = 0.00273\times10^{24}$ $N^O = 0.00558\times10^{24}$
Pressure shell	300	15.24	Ti	$N^{Ti} = 0.0566\times10^{24}$

[a]Unless otherwise noted, all materials are in volume percent.

[b]For 3.048-m- (10-ft-) cavity-diameter configuration.

[c]For 3.658-m- (12-ft-) cavity-diameter configuration.

[d]For 4.267-m- (14-ft-) cavity-diameter configuration.

[e]Composition based on pressure of 90.5 MN/m^2 (400 atm) used as the reference case.

[f]For some calculations the reflector contained heat-exchanger tubes made of separated Mo.

[g]For 0.457-m- (1.5-ft-) reflector-thickness configuration.

[h]For 0.61-m- (2-ft-) reflector-thickness configuration.

[i]For 0.762-m- (2.5-ft-) reflector-thickness configuration.

wall liner. Relatively cold hydrogen from a feed system fills a region adjacent to the cavity liner and flows into the high-temperature cavity. The reflector region contains heat-exchanger tubes to provide heat removal by helium coolant gas. The tube material was assumed to be the same as the reflector material, BeO, though metallic tubes were also considered. A coolant volume equivalent to 10.5 percent of the reflector volume was calculated to be sufficient to remove the heat generated by neutron and gamma absorption in the reflector material. Coolant volume fraction was assumed constant for all models and the calculated value of 10.5 percent was based on design limits of about 1.4-MN/m^2 (200-psi) pressure drop from inlet to outlet plenums and a 550 K (1000^{o} R) temperature rise between tubes. Plenums for the outlet and inlet coolant gas were located outside the reflector in order to keep reflector material as close to the core as possible. A foamed zirconium oxide insulation layer was provided to help protect the pressure shell from overheating. The titanium pressure vessel provided containment for the pressurized core materials. The rocket nozzle was neglected in the calculations because of its small size. (It was estimated to have a throat diameter of 3.8 cm, compared to a cavity diameter of about 3.7 m.)

Based on a previous survey, cavity diameters of 3.048 to 4.267 meters (10 to 14 ft) and reflector thicknesses of 0.457 to 0.762 meter (1.5 to 2.5 ft) appeared to be the range of interest. At lower diameters and reflector thicknesses the required containment pressure would be excessive (>101.4 MN/m^2, or 1000 atm). Region dimensions and compositions for the calculational model are itemized in table I. Thicknesses of all regions other than the cavity and the reflector are nominal and were selected as reasonable from the standpoints of fabrications and coolant pressure drop.

Temperatures in the hydrogen and fuel cavity regions were based on a heat transfer analysis of a 3.048-meter- (10-ft-) cavity-diameter reactor with a 0.457-meter (1.5-ft) reflector, operating at a pressure of 40.5 MN/m^2 (400 atm), and with a thrust of 196 600 newtons (44 200 lbf) and a specific impulse of 4400 seconds. This temperature profile was assumed to be applicable to all configurations studied herein. The average hydrogen temperature of 10 600 K represents the temperature corresponding to the average hydrogen atom in the cavity region and was obtained by volume averaging the product of temperature and density (see appendix A). At engine conditions, molecular hydrogen is largely dissociated. Theoretical data relating hydrogen density to temperature and pressure obtained by using the method described in reference 11 have been used to determine atomic densities of hydrogen for nuclear calculations.

The model described in table I was selected for the neutronics analysis even though some of the materials and region temperatures are still to be specified. For example, U^{238} was used as the propellant seed material primarily because vapor opacity data are available which are required in heat transfer calculations. Uranium-238 should be representative of the class of materials that could be used for this application. Also, the

temperatures of the cavity liner and feed hydrogen region were somewhat arbitrarily selected. Heat transfer analysis indicates that the cavity liner temperature is insensitive to propellant heating and therefore would probably be determined by the incoming hydrogen. This inlet temperature of the hydrogen could be adjusted over a reasonable range, depending on what, if any, heat load is imposed on it (e.g., nozzle and/or pressure vessel cooling) prior to entering the cavity liner.

Procedure

The calculational procedure was to select a reactor configuration and pressure and then calculate the critical mass. A fluid dynamics correlation was then used to determine whether the calculated critical mass could be contained by the assumed propellant pressure. If not, a new value for pressure was selected and the procedure was repeated.

Containment of fuel in an operating gas-core reactor must satisfy the following fluid dynamics criterion

$$P = 0.0038 \frac{M_F^{1.385} F^{0.383} I_{sp}^{0.383}}{D_c^{4.54} \left(\frac{V_F}{V_c}\right)^{1.51}} \tag{1}$$

where

P	cavity pressure, MN/m^2
M_F	fuel loading, kg
F	thrust, N
I_{sp}	specific impulse, sec
D_c	cavity diameter, m
V_F/V_c	volume fraction of fuel in cavity

This criterion is based on fluid dynamics and heat transfer conditions in the cavity. Equation (1) is based on a derivation in reference 7. The fuel mass must also meet the criterion of criticality, which for a parametric analysis is convenient to calculate in the form

$$M_c = M(\text{ref.}) - \left[\%\,\frac{\Delta k}{k}(\text{H press.}) + \%\,\frac{\Delta k}{k}(\text{H temp.}) + \%\,\frac{\Delta k}{k}(\text{structural material})\right]\frac{\Delta M}{\%\,\frac{\Delta k}{k}} \quad (2)$$

where

$M(\text{ref})$	critical mass of reactor with reference conditions, kg
$\%\,\frac{\Delta k}{k}(\text{H press})$	reactivity effect of hydrogen pressure, percent $\Delta k/k$
$\%\,\frac{\Delta k}{k}(\text{H temp})$	reactivity effect of using hydrogen temperature gradient in propellant region, percent $\Delta k/k$
$\%\,\frac{\Delta k}{k}(\text{structural material})$	reactivity effect of addition of structural material to reflector, percent $\Delta k/k$
$\frac{\Delta M}{\%\,\frac{\Delta k}{k}}$	reciprocal of fuel reactivity coefficient, kg/percent $\Delta k/k$

The reference critical mass M(ref.) is defined for calculational convenience as the critical mass of a gas-core reactor with hydrogen conditions of 40.5 MN/m^2 (400 atm) pressure and 10 600 K temperature and with no structural material in the reflector. Any reactor with these conditions is hereinafter referred to as a reference reactor, regardless of size.

For a given configuration, M_c was calculated based on estimated values for hydrogen pressure, hydrogen temperature, and structural material. Equation (1) was then utilized to evaluate whether the calculated M_c and the estimated hydrogen pressure P were consistent values for fuel containment. This procedure was iterated until $M_F = M_c$.

Criticality calculations were performed with the neutron transport code TDSN (ref. 12) using the S_4P_1 19-group options in spherical geometry. The notation scheme for code options can be described as follows: S_4 represents the angular quadrature scheme of order 4 for solving the S_n transport equations, P_1 represents cross sections obtained from a Boltzmann transport equation solution using the first two terms of a Legendre polynomial expansion, and 19-group signifies the number of discrete energy groups for which the multigroup transport equation will be solved. The use of S_4P_1 19-group options in neutron transport calculations was determined to be adequate for the criticality analysis of a heavy-water (D_2O)-reflected, gas-core (uranium hexafluoride) reactor critical experiment at room temperature (ref. 13). These code options were assumed to be applicable to the high-temperature reactor studied herein. Downscattering

was allowed between all groups, whereas upscattering was limited to the seven thermal energy ($E \leq 2.38$ eV) groups.

Neutron cross sections were generated with the GAM-II (ref. 14) and GATHER-II (ref. 15) codes. Twelve fast group cross sections ($E > 2.38$ eV) were flux weighted over a U^{235} slowing-down spectrum for use in the core region and over a BeO spectrum for use in all regions outside the core. Seven thermal group cross sections ($E \leq 2.38$ eV) were flux weighted over a BeO spectrum at 1600 K for use in all reactor regions. Also, the nuclei in each region were assumed to be at their appropriate temperature in an operating engine. The use of high-temperature nuclei in the calculation (as opposed to no temperature correction) significantly increased the hydrogen scattering cross sections. At equivalent temperatures the velocity of protons (atomic hydrogen) is equal to that of neutrons. Since the cross section, or probability of reaction, is a strong function of the relative velocity between a proton and a neutron, this effect is particularly important in the cavity of a gas-core reactor, where protons can exist at temperatures of the order of 30 000 K. The GATHER II code was used to calculate free gas scattering kernels for fuel and hydrogen regions. The resulting cross sections are then flux weighted over the spectrum of interest, in this case BeO at 1600 K.

DESIGN PROCEDURE

Reactivity effects of the major variables of hydrogen pressure, hydrogen temperature, and percentage of structural material were calculated for a range of conditions. These reactivity effects were transformed to required changes in fuel loading by the use of fuel reactivity worths. The reference reactor critical mass was adjusted with the calculated change in fuel loading to obtain the critical mass for a given configuration.

Reference Reactor Calculations

To provide a basis for critical mass determinations, criticality calculations were performed for cavity diameters of 3.048, 3.658, and 4.267 meters (10, 12, and 14 ft) and for reflector thicknesses of 0.457, 0.610, and 0.762 meter (1.5, 2.0, and 2.5 ft). Hydrogen conditions in the cavity were assumed to be 40.5 MN/m^2 (400 atm) and 10 600 K. The fuel was uniformly distributed within the core region, which was assumed to be the central 30 percent of the cavity volume. No mixing was assumed to occur between fuel and hydrogen in the cavity.

Critical fuel density is shown in figure 2 to decrease with increasing cavity diameter (or core diameter) and with increasing reflector thickness. However, total fuel loading increases with increasing cavity diameter (fig. 3).

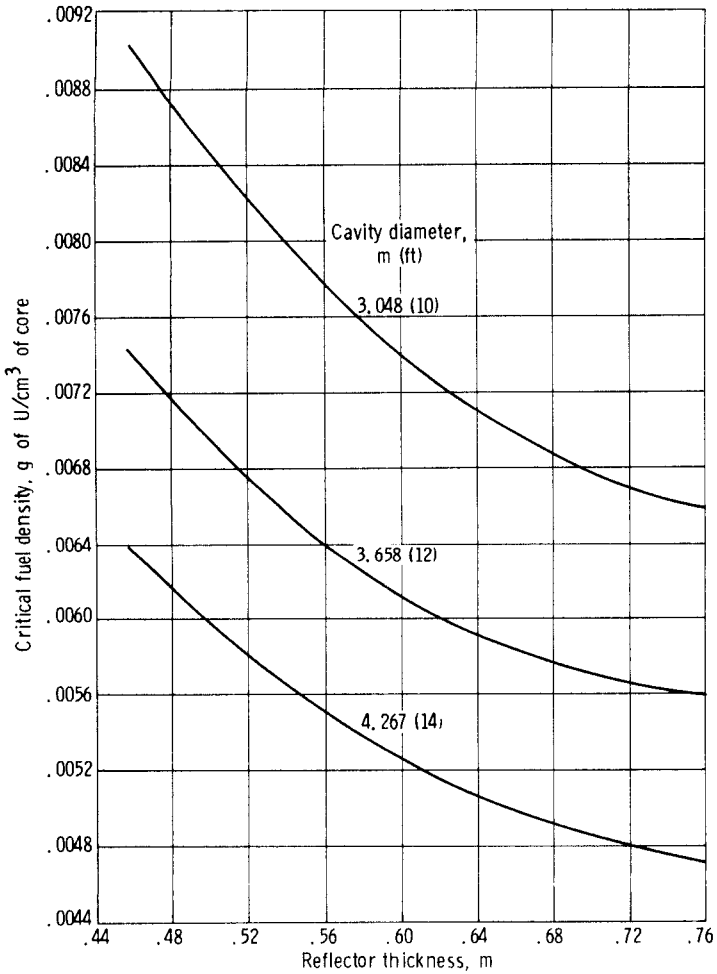

Figure 2. - Critical fuel density of reference reactor configuration with propellant hydrogen at 40.5 MN/m^2 (400 atm) and 10 600 K.

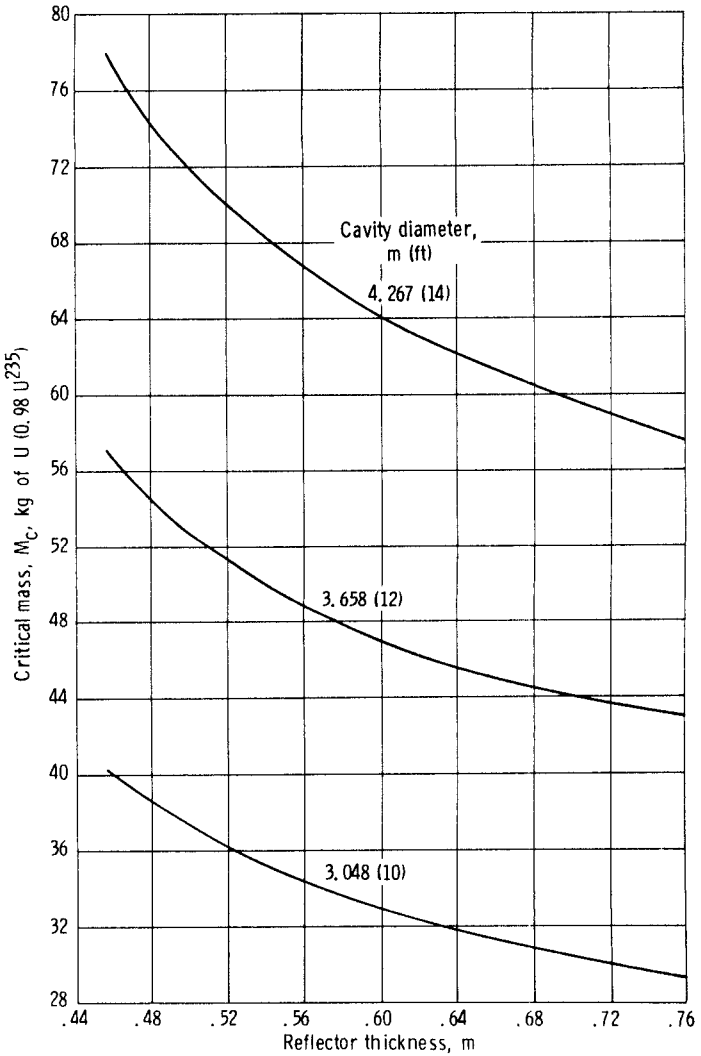

Figure 3. - Critical mass of reference reactor configuration with propellant hydrogen at 40.5 MN/m^2 (400 atm) and 10 600 K.

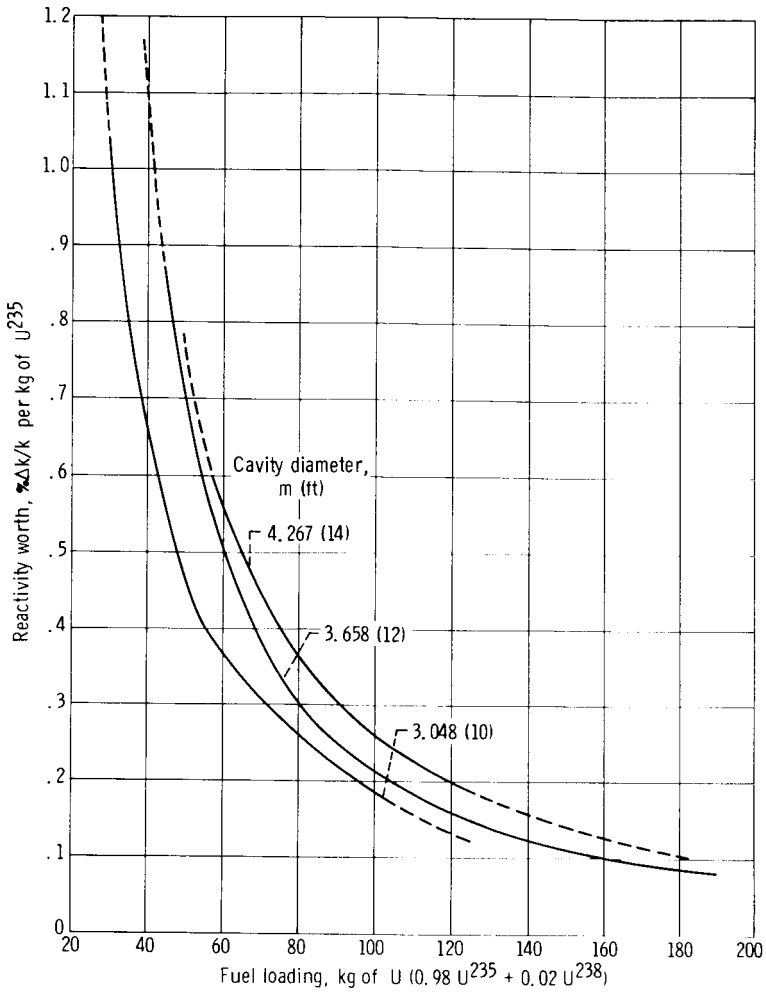

Figure 4. - Fuel reactivity worth for gas-core reactors.

Fuel reactivity worths were determined for a wide range of fuel loadings with cavity diameter as a parameter (fig. 4). At the higher fuel loadings the analytical model contained structural material in the reflector region, and at lower fuel loadings the reference reactor was used. However, the correlation appeared to be consistent, thus indicating fuel worth as a function of fuel loading to be essentially independent of material variations external to the reactor cavity. The general shape of the curves has been obtained experimentally on a D_2O-moderated gas-core critical mockup (ref. 16).

Hydrogen Conditions

The hydrogen in the reactor cavity region, because of its location between the fuel and the reflector, significantly affects the multiplication factor. Neutrons which have

been thermalized in the reflector and then returned to the fuel region are the major source of reactivity. However, while passing through the hydrogen, these neutrons are subject to both absorption and scattering collisions. Absorption reduces fission probability by capturing the neutron before it can reach a fissionable atom. Scattering can affect criticality by changing the path of the neutron and by changing the energy of the neutron, thereby either reducing or enhancing its fission probability depending on the energy dependence of the fission cross section. If the hydrogen is hot (at energies greater than thermal), the tendency is to upscatter the neutrons, that is, transfer energy from protons (atomic hydrogen) to neutrons at lower energy levels. The near-Maxwellian distribution of neutrons emanating from the reflector is thus hardened (increased in energy) before it reaches the fuel. The effect is to reduce criticality by upscattering the neutrons into an energy range where the probability of capture (parasitic absorption) relative to fission in the fuel is greater than at lower energies.

The actual hydrogen cavity pressure is a function of the fuel mass (eq. (1)). Therefore, to generalize the reference reactor critical masses, the reactivity effect was calculated by substituting hydrogen at 20.3, 81.1, and 121.6 MN/m^2 (200, 800, 1000 atm) into the cavity of reactor. The resulting change in reactivity is plotted in figure 5. For these calculations the hydrogen density as a function of pressure was obtained from figure 14 (discussed in appendix B). Increasing slope (rate of reactivity change per unit pressure) with increasing cavity diameter results from the greater width of the cavity hydrogen region. (For all configurations the ratio of fuel diameter to cavity diameter was 0.67.) This greater width allows more proton-neutron collisions for a given pres-

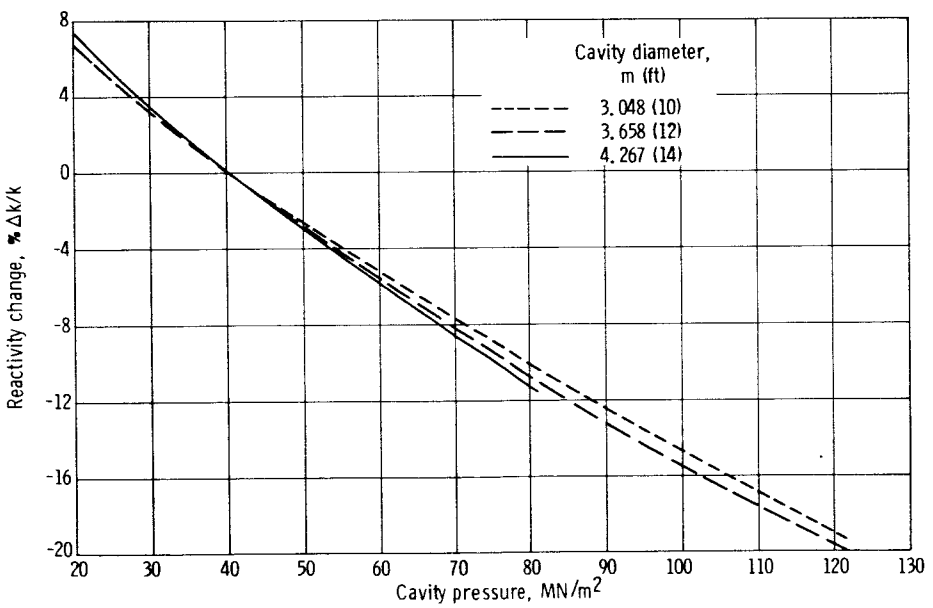

Figure 5. - Reactivity effect of hydrogen pressure in reference reactor configuration.

sure. Neutron absorption in cavity hydrogen as a function of pressure is shown in table II to vary almost proportionately with pressure. The reactivity effect is compounded, however, by the fact that this absorption selectively removes low-energy neutrons, thereby hardening the neutron spectrum before it enters the fuel region. As a result the median fission energy, which was 0.31 electron volt at 20.3 MN/m^2 (200 atm), increased to 0.72 electron volt at 121.6 MN/m^2 (1200 atm). Greater parasitic absorption in the fuel as the spectrum hardens is illustrated by the ratio of neutron captures to fissions increasing from 0.226 to 0.234 as hydrogen pressure increases from 20.3 to 121.6 MN/m^2 (200 to 1200 atm).

TABLE II. - EFFECT OF CAVITY PRESSURE ON CORE FLUX SPECTRUM FOR REACTOR

[Cavity diameter, 3.658 m (12 ft); reflector thickness, 0.609 m (2 ft); hydrogen temperature, 10 600 K.]

Cavity pressure		Median fission energy, eV	Ratio of neutron captures to fissions in fueled region	Absorption in cavity hydrogen region per source neutron
MN/m^2	atm			
20.3	200	0.31	0.226	0.0075
40.5	400	.39	.229	.0156
81.1	800	.60	.231	.0325
121.6	1200	.72	.234	.0490

All previous calculations in this report have contained the simplifying assumption of a uniform hydrogen cavity temperature. However, in an operating engine a gradient will exist between the relatively hot hydrogen-fuel interface and the cool hydrogen - cavity liner boundary. The calculated temperature distribution in the cavity hydrogen, shown in figure 6, decreases from 26 300 K at the fuel interface to 1600 K at the cavity liner. Any variation of hydrogen temperature with cavity diameters and pressures was assumed to be sufficiently small that the data in figure 6 were applied to all configurations considered herein. For calculational purposes the hydrogen region was represented by five spherical shells ranging in temperature from 4160 to 22 400 K (appendix A).

The reactivity effect of zoning the hydrogen was -0.25 percent $\Delta k/k$ for a 3.048-meter- (10-ft-) diameter, 0.61-meter- (2.0-ft-) thick reflector configuration (case 1) and -0.50 percent $\Delta k/k$ for a 3.658-meter- (12-ft-) diameter, 0.61-meter- (2-ft-) thick reflector configuration (case 2). Spectral and criticality data for these two cases are compared to the uniform 10 600 K hydrogen calculations in table III. The negative reactivity effect is seen to come from increased neutron-capture-to-fission ratios in the fuel.

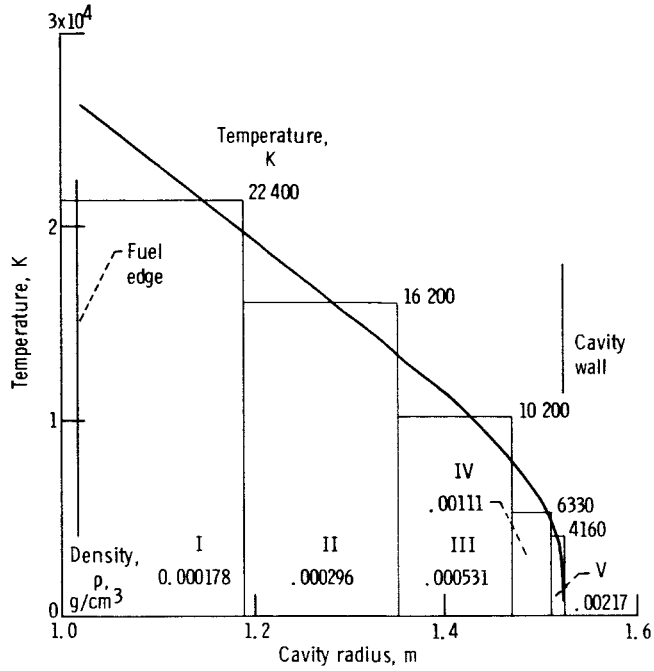

Figure 6. - Calculational model representation of hydrogen temperature distribution in cavity of gas-core reactor. Cavity diameter, 3.048 meters (10 ft); pressure, 40.5 MN/m^2 (400 atm); thrust, 196 600 newtons (44 200 lbf); specific impulse, 4400 seconds.

TABLE III. - EFFECT OF HYDROGEN TEMPERATURE DISTRIBUTION ON CORE PROPERTIES

Core property	Cavity diameter, 3.658 m (12 ft); reflector thickness, 0.61 m (2 ft)		Cavity diameter, 3.048 m (10 ft); reflector thickness, 0.61 m (2 ft)	
	Hydrogen zone at 10 600 K average temperature[a]	Hydrogen separated into five zones (fig. 6)	Hydrogen zone at 10 600 K average temperature[a]	Hydrogen separated into five zones (fig. 6)
Multiplication factor	1.0039	0.9988	0.9995	0.9970
Median fission energy, eV	0.39	0.37	0.36	0.34
Ratio of neutron captures to fissions in fueled region	0.229	0.236	0.227	0.234
Absorptions in cavity hydrogen region per source neutron	0.0156	0.0165	0.0127	0.0133
Reactivity worth of zoning, $\% \Delta k/k$	-0.50	-0.50	-0.25	-0.25

[a]Temperature corresponding to average hydrogen density in cavity.

Since the five-zone hydrogen case has regions at temperatures both above and below the uniform 10 600 K calculation, both hardening and softening of the flux spectrum occurs. The result is to broaden the low-energy distribution (fig. 7). The net effect on median fission energy (table III) was a reduction of 0.02 electron volt. However, the greater importance of the upscattered neutrons on criticality is indicated by an increase in fuel-capture-to-fission ratio.

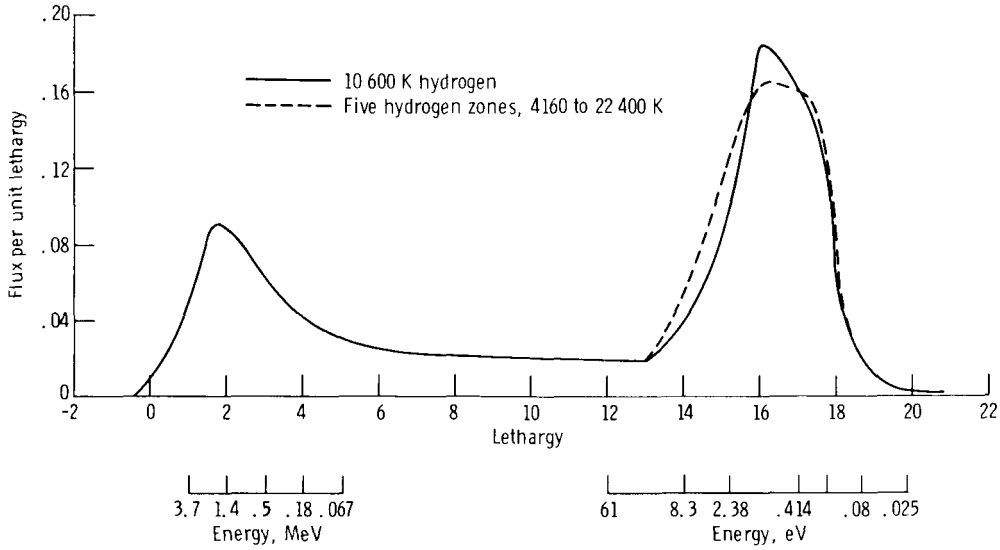

Figure 7. - Normalized flux spectra at hydrogen-fuel interface. $\Phi = \int_{-0.4}^{\infty} \varphi(u)du = 1$.

The small reactivity decrease due to hydrogen zoning indicates the adequacy of using the temperature of an average hydrogen atom in the propellant cavity region. This average is obtained by volume averaging the product of density times temperature of the hydrogen. Also, total hydrogen atoms are conserved.

Structural Materials

Scoping calculations indicated that the gas-core reactor was sufficiently sensitive to neutron absorber materials that no standard structural material with acceptable high-temperature properties could be used in practical quantities. Thus, the proposed structural material was separated molybdenum (Mo) which would be used in the alloy TZM. The Mo would be isotopically enriched to >98 percent of Mo^{98} and Mo^{100} in order to reduce the low-energy neutron absorption cross section to as low a value as possible based on the difficulties (and cost) associated with the separation process. The actual isotopic

distribution used was not included because of classification of production data.

Results of criticality calculations on various reactor configurations indicated that the relative critical mass as a function of Mo content in the reflector-moderator was nearly independent of cavity diameter and of reflector thickness (table IV). Relative critical mass is defined as the ratio of the critical mass for a reactor configuration with a given Mo content to the critical mass for that same configuration with no Mo in the reflector-moderator. Initial calculations using 1.7-volume-percent niobium in the reflector indicated that relative critical mass varied from 2.59 to 2.73 as reflector thickness varied from 0.457 meter (1.5 ft) to 0.762 meter (2.5 ft). Later calculations using 3.035-volume-percent separated Mo showed that relative critical mass varied from 1.64 to 1.62 as cavity diameter varied from 3.658 meters (12 ft) to 4.267 meters (14 ft). These

TABLE IV. - STRUCTURAL MATERIAL EFFECT ON CRITICAL MASS AS FUNCTION OF CAVITY DIAMETER AND REFLECTOR THICKNESS

Structural material	Content in reflector, vol %	Cavity diameter		Reflector thickness		Relative critical mass
		m	ft	m	ft	
Niobium	1.7	3.658	12	0.4512	1.5	2.59
	1.7	3.658	12	.61	2.0	2.68
	1.7	3.658	12	.762	2.5	2.73
Separated molybdenum[a]	3.035	3.658	12	0.61	2.0	1.64
	3.035	4.267	14	.61	2.0	1.62
	6.07	3.658	12	.61	2.0	2.68

[a]Greater than 98 percent Mo^{98} and Mo^{100}.

values were judged sufficiently constant to warrant a single correlation for relative critical mass against volume percent material which would include all cavity diameters and reflector thicknesses in this study. Such a correlation for separated Mo is presented in figure 8 for a range to 6.07 percent.

The upper limit of 6.07 percent was selected because this allows enough material to construct heat-exchanger tubes that could withstand 40.5-MN/m^2 (400-atm) external pressure (ref. 5). At higher material percentages the increase in critical mass appears to exceed the range of interest for design purposes.

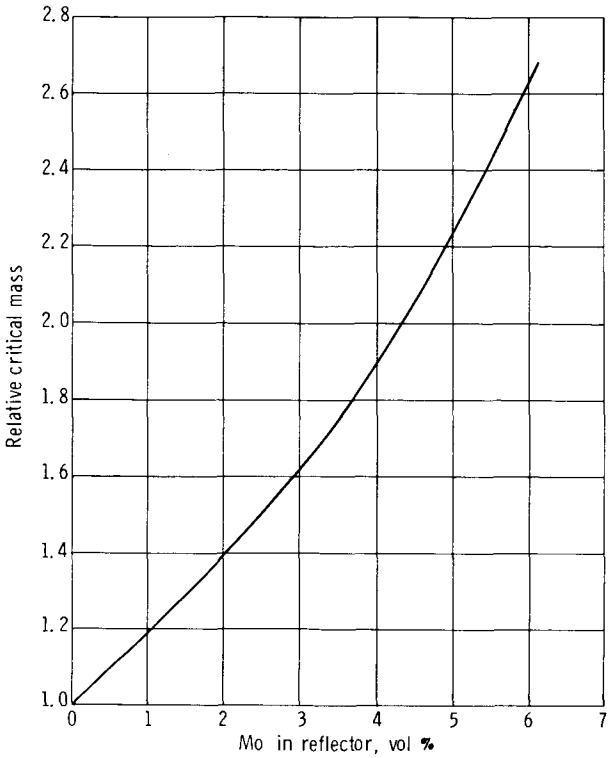

Figure 8. - Effect on critical mass resulting from separated molybdenum being added homogeneously to reflector of reference reactor configuration.

Example Calculation

To obtain the fuel mass for a specific configuration both the criteria stated in equation (1) for containment conditions and in equation (2) for criticality must be satisfied. The reference configuration critical mass can be adjusted by the use of reactivity coefficients developed in the previous sections to arrive at a fuel mass and hydrogen pressure consistent with the amount of structural material contained in the reflector. In order to utilize the structural material correlation in figure 8, equation (2) was rearranged as follows

$$M_c = M(\text{ref.}) \times R - \left[\%\,\frac{\Delta k}{k}\,(\text{H press.}) + \%\,\frac{\Delta k}{k}\,(\text{H temp.})\right]\frac{\Delta M}{\%\,\frac{\Delta k}{k}} \qquad (3)$$

where R equals the relative critical mass factor caused by structural material.

Both hydrogen pressure and fuel mass are unknown initially. Once the cavity diameter, reflector thickness, and amount of structural material have been set, an iterative

procedure is required until consistent values are obtained. Equation (3) is solved for the appropriate values of M(ref.), R, and H(temp.) by using an estimated hydrogen pressure. The resulting M_c is then substituted into equation (1) to obtain the hydrogen pressure P required for containment. If necessary, this procedure is iterated until P agrees with the estimated hydrogen pressure.

An example problem follows for a 4.267-meter- (14-ft-) cavity-diameter, 0.61-meter- (2.0-ft-) reflector-thickness configuration containing 1.9-percent separated Mo in the reflector region:

$$M(\text{ref.}) = 63.6 \text{ kg (fig. 3)}$$

$$R = 1.38 \text{ (fig. 8)}$$

$$\% \frac{\Delta k}{k}(\text{H temp.}) = -0.65 \text{ (derived from table III)}$$

The pressure is estimated to be 50.7 MN/m^2.

$$\% \frac{\Delta k}{k}(\text{H press.}) = -3.1 \text{ (fig. 5)}$$

$$M_c = 63.6 \times 1.38 + (0.65 + 3.1) \% \frac{\Delta k}{k} \frac{\Delta M}{\% \frac{\Delta k}{k}} = 87.8 + 3.75 \% \frac{\Delta k}{k} \times \frac{\Delta M}{\% \frac{\Delta k}{k}} \qquad (3)$$

By using figure 3, the 4.267-meter curve is integrated from 87.8 kilograms to some value of M_c at which the area under the curve equals about 3.75 percent $\Delta k/k$. Thus, $M_c = 87.8 + 3.75 \frac{14.2}{3.91} = 87.8 + 13.6 = 101.4$ kg.

$$P = 0.0038 \frac{(101.4)^{1.385}(196\,600)^{0.383}(4400)^{0.383}}{(4.267)^{4.54}(0.3)^{1.51}} \qquad (1)$$

$$= 0.0854\,(101.4)^{1.385} = 51.2 \text{ MN/m}^2$$

Since 51.2 MN/m^2 exceeds the estimated pressure, the pressure is reestimated to be 55.8 MN/m^2.

$$\% \frac{\Delta k}{k} (\text{H press.}) = -4.6 \text{ (fig. 5)}$$

$$M_c = 87.8 + 5.25 \frac{20.2}{5.32} = 87.8 + 19.9 = 107.7 \text{ kg}$$

$$P = 0.0854 \ (107.7)^{1.385} = 55.8 \text{ MN/m}^2$$

Since the calculated pressure equals the estimated pressure, the hydrogen pressure will contain the fuel mass.

As a check on this method, this configuration was calculated directly. The calculated k of 1.0087, compared to k = 1.0, indicated the adequacy of treating the parametric effects of pressure, temperature, and structural material independently.

Calculated Critical Mass

Predicted reactor conditions of critical fuel mass and hydrogen pressure are quite sensitive to the accuracy of the calculated multiplication factor k, due to the low net reactivity worth of fuel over much of the design range. The significant effect of a few percent in k on the design conditions of a 3.658-meter- (12-ft-) diameter reactor with a 0.61-meter- (2.0-ft-) thick reflector is shown in figure 9. As k varies from 1 to 1.05, critical mass varies from 44.3 to 58.2 kilograms and hydrogen pressure from 32.9 to 48.1 MN/m^2 (325 to 475 atm). Constant-pressure lines are included in figure 9 to indicate the lesser effect on critical mass if the corresponding hydrogen pressure increase is not considered in the calculations. The relative change in critical mass increases as design pressure increases because of the lower net reactivity effect discussed previously and tabulated in table V.

A possible bias in the criticality calculations of a few percent could come from a number of sources. Critical experiments were necessarily performed at lower temperatures, thereby omitting the reactivity effect of a hot hydrogen region between the fuel and the reflector. This analysis has shown that the resulting effect of high-energy hydrogen atoms on k is substantial due to spectrum hardening. Various potential sources of error in this study and their estimated effect on k are itemized in table VI. It is impossible to estimate with any confidence the net effect of these phenomena, although the potential exists (in either direction) for a major change in the numerical results of this study.

Also neglected in this analysis is excess reactivity which would be required by a reactor control system. This could be of the order of 4 or 5 percent $\Delta k/k$. If desired, excess reactivity could be included in the design procedure described herein by requiring

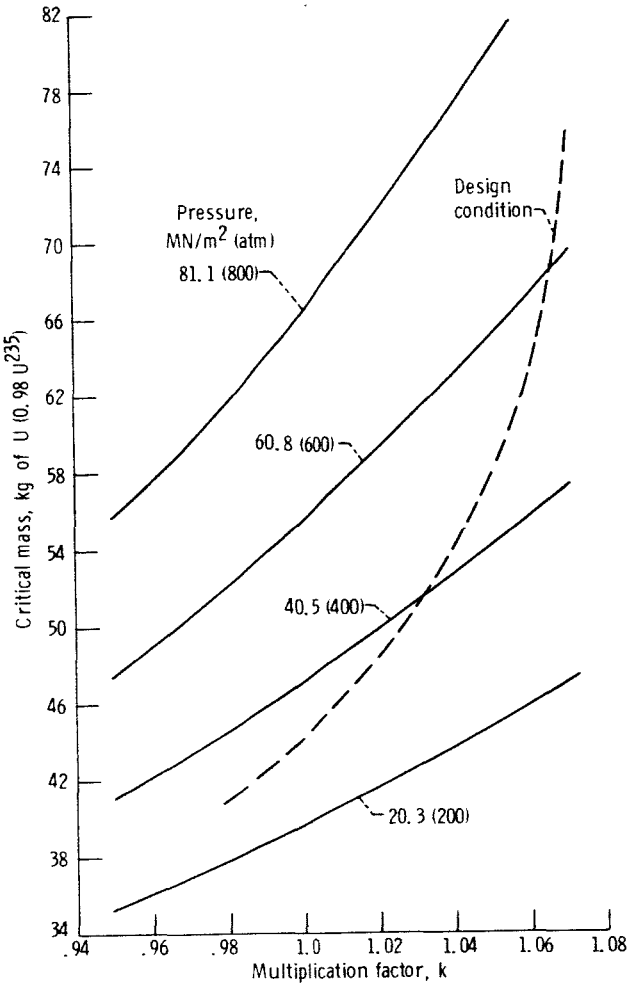

Figure 9. - Effect of calculated multiplication factor on critical mass in reference reactor configuration. Cavity diameter, 3.658 meters (12 ft); reflector thickness, 0.61 meter (2 ft).

TABLE V. - NET REACTIVITY WORTH OF INCREMENTAL FUEL ADDITION TO GAS CORE REACTOR

[Cavity diameter, 4.267 m (14 ft); thrust, 196 600 N (44 200 lbf); specific impulse, 4400 sec.]

Fuel mass, kg	Cavity pressure		Fuel worth, $\frac{\% \Delta k/k}{kg\ U^a}$	Hydrogen worth			Net reactivity worth, $\frac{\% \Delta k/k}{kg\ U^a}$
	N/m^2	atm		$\frac{MN/m^2\ H}{kg\ U^a}$	$\frac{\% \Delta k/k}{MN/m^2\ H}$	$\frac{\% \Delta k/k}{kg\ U^a}$	
50	19.3	190	0.76	0.54	0.40	0.21	+0.55
60	24.7	244	.56	.60	.40	.24	+0.32
80	37.0	365	.35	.65	.34	.22	+0.14
100	50.1	495	.26	.70	.30	.21	+0.05
110	57.2	565	.23	.72	.30	.21	+0.02
120	64.9	640	.20	.75	.28	.21	-0.01
140	80.1	790	.16	.80	.26	.21	-0.05

[a]Total uranium (0.98 U^{235} + 0.02 U^{238}).

TABLE VI. - POSSIBLE UNCERTAINTIES IN CRITICALITY CALCULATIONS

Phenomenon	Comment	Estimated change in reactivity, $\Delta k/k$
Beryllium cross sections	Possibly inaccurate based on previous reactor analyses; e.g., fast critical experiments (ref. 18) and the Tungsten Water Moderated Reactor program at Lewis Research Center.	-6 to +2 percent.
Transport code options P order, energy groups, mesh spacing	Original calculation technique established for a cold, heavy-water (D_2O)-reflected reactor without atomic hydrogen. Upscattering caused by high-temperature hydrogen indicates that more energy groups are needed in the eipthermal range.	Possibly a few percent either way.
Reactivity coefficient interdependence	Design procedure is based on independent effects of hydrogen temperature, hydrogen pressure, and structural materials. The degree to which this is wrong will affect k.	Possibly a few percent either way.
Fission products	Xenon-135 buildup has been neglected.	About -0.8 percent.
Material impurities	Reactor-grade beryllium oxide can contain up to a few hundred ppm of impurities.	Up to a few percent negative.
Fuel shape	Although a spherical shape was assumed, experimental data indicate that it would probably be closer to a teardrop.	Undetermined.
Fuel-propellant boundary layer mixing	Although a well-defined boundary was assumed, diffusion and mixing will probably occur.	Undetermined.
Fuel-diameter-to-cavity-diameter ratio	Criticality calculations are sensitive to this value, which has not been well defined experimentally.	Significant either way.

that the critical mass and pressure correspond to k excess instead of k = 1.

The calculational model used herein to represent a gas-core reactor is based on today's best guess of reactor conditions. However, it should be recognized that the calculated data in this study are particularly sensitive to the fuel-diameter-to-cavity-diameter ratio, which is probably known with less accuracy than any other reactor condition. If the fuel-diameter-to-cavity-diameter ratio were larger than 0.67, reactivity would increase both because more fuel would be in the cavity and because less hydrogen would be in the cavity. Increased reactivity could be translated into a lower critical fuel loading for a given reactor configuration. Of course, the converse would be true if the fuel-diameter-to-cavity-diameter ratio were less than 0.67.

The calculational model was based on complete separation of fuel and propellant primarily because of a lack of fluid mechanics information. Based on qualitative experimental results a more realistic analytical model would include propellant within the fuel region. Some propellant could permeate the entire fuel region, and it is probable that a transition region of fuel and propellant exists between the separate flow regions. The reactivity effect of hydrogen inside the fuel region is positive. However, for a given fuel loss rate the net effect of hydrogen dilution on pressure is not known. Consequently, the phenomenon is recognized in this study but no attempt has been made to evaluate the effect on required fuel loading.

CORE CHARACTERISTICS

Ancillary results were derived from the study required for development of the aforementioned design procedure relating critical mass to propellant pressure. These data are presented in this section.

Limiting Pressure

Inspection of equations (1) and (3) indicates that any addition of fuel to a subcritical configuration also requires the addition of hydrogen through increased pressure. Thus, the net reactivity effect (positive fuel reactivity and negative hydrogen reactivity) would be a better indication of real fuel worth to a design. As the fuel loading of a reactor increases, the reactivity worth of the fuel decreases rapidly; however, hydrogen worth is relatively constant. Consequently, the net reactivity effect decreases at a faster rate (table V). These data indicate that there is some pressure above which fuel is worth so little that the net reactivity effect of adding fuel is negative. Above this fuel loading (or propellant pressure) a critical engine cannot be obtained without the use of some control system. For example, above this limiting pressure the addition of fuel makes the reactor more subcritical because the negative worth of the hydrogen required to contain the fuel mass is greater than the positive worth of the fuel. Figure 10 shows the limiting pressure for 3.048-, 3.658-, and 4.267-meter- (10-, 12-, and 14-ft-) diameter reactors to be 75, 69, and 62 MN/m^2 (720, 680, and 610 atm), respectively. Of course, these results apply only to the range studied herein. It is conceivable that the reactivity worth curves in figure 10 could become positive at a much higher pressure, where the hydrogen region might act as a reflector.

The preceding analysis was based on a reactor with no reactivity margin for a control system. A similar analysis with excess reactivity would lead to larger limiting pressures.

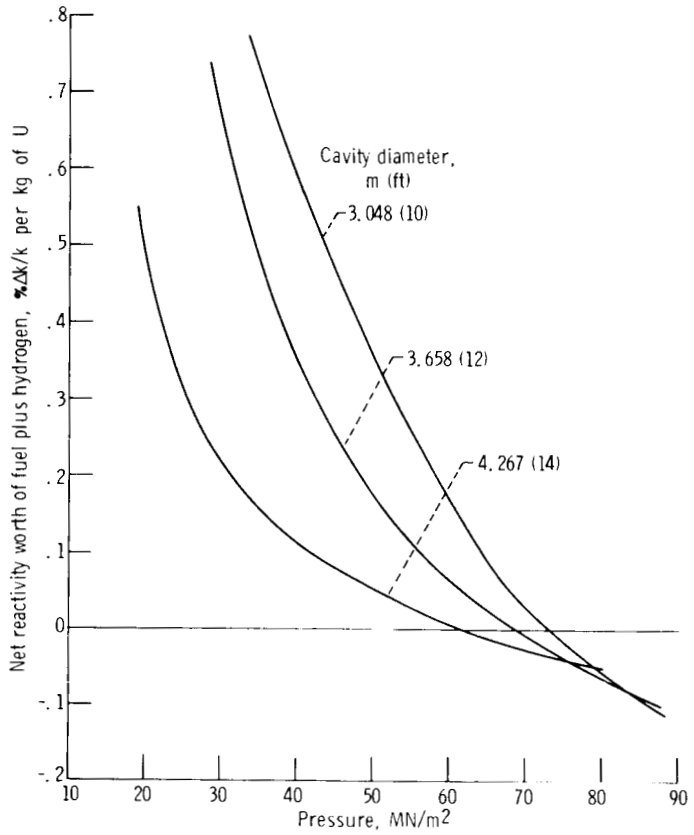

Figure 10. - Net specific reactivity worth of fuel addition to reference reactor configuration. Thrust, 196 600 newtons (44 200 lbf); specific impulse, 4400 seconds.

Hydrogen Upscattering and Temperature Effects

As indicated previously, the upscattering of neutrons by high-temperature hydrogen atoms can be expected to reduce criticality. The magnitude of this effect was investigated by performing a criticality calculation using a special set of hydrogen cross sections. This set included the same fast group cross sections as used in reference calculations, but the thermal group microscopic cross sections were generated at 1600 K instead of 10 600 K. The macroscopic cross-section set was calculated from a hydrogen density corresponding to 10 600 K. This procedure maintained the same absorption probability (density dependence) as the reference calculations but isolated the upscattering effect (temperature dependence). The results in table VII indicate that the upscattering effect of 10 600 K hydrogen is worth about -15 percent $\Delta k/k$ compared to 1600 K hydrogen. The negative worth results directly from the relatively greater capture probability in the fuel at higher temperatures (energies) and is indicated by the increase from 0.218 to 0.229 of the ratio of neutron captures to fissions in the fuel region. The significance of

TABLE VII. - EFFECT OF HYDROGEN UPSCATTERING ON CRITICALITY OF GAS-CORE REACTOR

[Cavity diameter, 3.658 m (12 ft); reflector thickness, 0.61 m (2.0 ft); pressure, 40.5 MN/m^2 (400 atm).]

Treatment of hydrogen	Multiplication factor	Ratio of neutron captures to fissions in fuel
Thermal group microscopic cross sections at 1600 K (density for macroscopic cross sections based on 10 600 K)	1.1878	0.218
10 600 K microscopic and macroscopic cross sections (reference calculations)	1.0039	.229
Zoned regions (4160 to 22 400 K microscopic cross sections with corresponding densities)	.9988	.236

the upscattering worth of hot hydrogen to reactor design becomes apparent when compared to the previous section on the sensitivity of calculations to variations in k.

The effect of hydrogen upscattering on criticality led to consideration of whether low-temperature hydrogen would offer a sufficiently lower fuel mass (and therefore lower weight) to warrant a lower specific impulse design. Calculations were performed with cavity hydrogen at 1600, 10 600, and 22 400 K and a constant pressure of 40.5 MN/m^2 (400 atm). The resulting data, itemized in table VIII, show that the lower critical mass

TABLE VIII. - EFFECT OF HYDROGEN TEMPERATURE ON CORE PROPERTIES FOR GAS-CORE REACTOR

[Cavity diameter, 3.658 m (12 ft); reflector thickness, 0.61 m (2 ft); cavity pressure, 40.5 MN/m^2 (400 atm).]

Core property	Hydrogen average temperature, K		
	1600	10 600	22 400
Critical mass, kg	~65.6	46.5	47.4
Neutron absorptions in cavity hydrogen per source neutron	~0.204	0.0156	0.0057
Mean fission energy, eV	~0.21	0.39	0.30
Ratio of neutron captures to fissions in fuel	~0.210	0.229	0.254

occurred at 10 600 K and that only a slight weight penalty was incurred by raising the propellant temperatures to 22 400 K. However, in an operating engine this high-temperature weight penalty would be magnified. As propellant temperature is increased, the specific impulse increases and, as a result, the propellant pressure required to contain a given fuel mass increases (see eq. (1)). Greater hydrogen pressure would increase critical mass. The opposite argument can be made to show that the weight penalty in the 1600 K case is less than that calculated at constant pressure. To determine fuel mass as a function of propellant temperature would have required establishing a fuel-propellant pressure relationship at each temperature of interest, and that was considered beyond the scope of this report.

At 1600 K, neutron absorption in the cavity hydrogen region was dominant; and at 22 400 K, the upscattering of neutrons by the cavity hydrogen produced increased neutron capture in the fuel. The higher density of hydrogen at 1600 K (a factor of 13 higher than 10 600 K) caused neutron absorption in the cavity hydrogen to increase from 1.7 to 22.2 percent of the source neutrons. The lower density of hydrogen at 22 400 K caused a reduction in neutron absorption (increased reactivity), but this effect was negated by the increased fuel-capture-to-fission ratio of upscattered neutrons. These data are not intended to indicate that the 10 600 K hydrogen is the best case but only to show the trend that neutron absorption becomes important at low temperatures and neutron energy level (or spectrum) becomes important at high temperatures.

The decrease in median fission energy at a propellant temperature of 22 400 K appears anomalous until one considers that several competing reactions are taking place - absorption, downscattering, and upscattering. Spectra at the fuel-hydrogen interface are plotted in figure 11 for propellant temperatures of 1600, 10 600, and 22 400 K. The high-energy peaks at about 2 MeV are neutrons from fissions in the core, and the low-energy peaks at 0.2 to 2 electron volts are neutrons which have been thermalized in BeO and hydrogen and returned to the core. Spectrum hardening due to temperature should shift the low-energy peaks toward higher energies as temperature increases. However, at constant pressure the hydrogen density decreases with increasing temperature, thereby allowing more low-energy neutrons to reach the core. When collisions do occur in higher temperature hydrogen, neutrons are upscattered to higher energies. This could explain the shape of the 22 400 K curve in which more low-energy and more high-energy neutrons occur than at 10 600 K. The net effect could be to lower mean fission energy. At 1600 K sufficient downscattering apparently occurs in neutron-proton collisions to more than compensate for absorption of low-energy neutrons.

The hump in the 22 400 K spectrum in figure 11 at a lethargy of about 14 is not a real phenomenon but instead represents a calculation problem. The GATHER-II code used to generate microscopic cross sections has an upper energy cutoff of 2.38 electron volts. Therefore, all upscattering reactions which cause the scattered neutron energy to exceed 2.38 electron volts are lumped into the next higher energy group (2.38 to 8.32 eV) instead

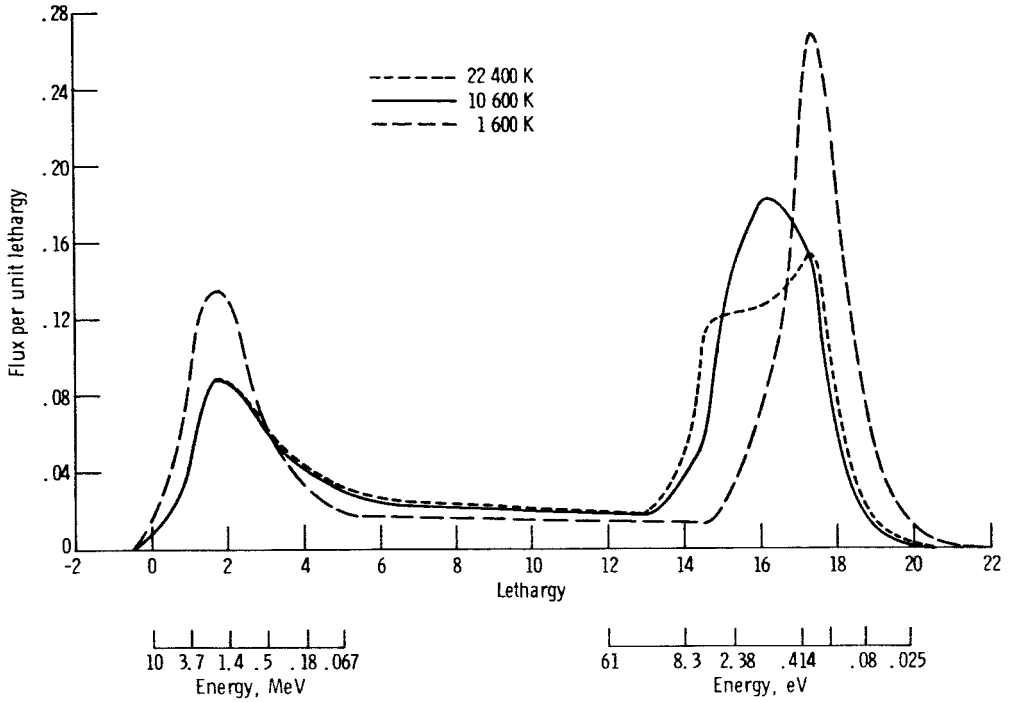

Figure 11. - Flux spectra at fuel-hydrogen interface in reference reactor configuration with constant-temperature hydrogen in cavity at 40.5 MN/m^2 (400 atm). $\Phi = \int_{-0.4}^{\infty} \varphi(u)du = 1$.

of being distributed to their proper energy. For calculations at 10 600 K or lower, so few neutrons were scattered above 2.38 electron volts that this procedure did not affect the transport calculation. At 22 400 K, however, a significant population of neutrons occurs in the 2.38- to 8.32-electron-volt group. Better upscattering cross sections would tend to spread the neutrons out to higher energies, thereby smoothing out the curve in figure 11. The effect on reactor calculations using U^{235} fuel would probably be to increase the multiplication factor because the average neutron energy would increase into an energy range where the ratio of capture to fission cross section decreases. (An absorption resonance in the group above the cutoff energy results in a large capture-to-fission ratio in that energy range.) The effect on reactor calculations with other fuels would depend on the behavior of their fission and absorption cross sections in the 2- to 20-electron-volt energy range. In this study, however, the magnitude of any effect on k should be quite small because so few neutrons are affected in the reference configuration calculations (fig. 7).

Reactivity Coefficients

A number of reactivity coefficients were calculated for the gas-core reactor to support a reactor dynamics study. These data, itemized in table IX, have been reduced to

TABLE IX. - CALCULATED REACTIVITY COEFFICIENTS FOR KINETICS ANALYSIS OF GAS-CORE REACTOR

Property	Calculated range			Formula
	Limits		Mean value	
	Lower	Upper		
Fuel mass, kg[a]	42	47	44.5	$\Delta k/k = 0.38\ (\Delta M/M)$
Fuel temperature, K	50 000	60 000	55 000	$\Delta k/k = 0.001\ (\Delta T/T)$
Fuel radius, cm[b]	122.6	137.1	129.85	$\Delta k/k = 0.21\ (\Delta R/R)$
Propellant mass, kg[c]	8.7	26.6	17.6	$\Delta k/k = -0.19\ (\Delta M/M)$
Propellant temperature, K	1600	10 600	6100	$\Delta k/k = -0.11\ (\Delta T/T)$
	10 600	16 200	13 400	$\Delta k/k = -0.24\ (\Delta T/T)$
Moderator temperature, K	1600	1700	1650	$\Delta k/k = -0.018\ (\Delta T/T)$

[a]Value is for 3.658-m- (12-ft-) cavity-diameter configuration. Coefficient varies with fuel loading and cavity diameter. Other values can be calculated from data in fig. 4.

[b]Represents D_F/D_c variation of 0.67 to 0.75.

[c]Corresponds to a pressure of 81.1 MN/m^2 (800 atm).

the standard form $\Delta k/k = F \times \Delta p/p$, where F is the coefficient and $\Delta p/p$ is the relative change of some property. Care must be taken, however, in interpreting the data because the coefficients have been specifically tailored for use in gas-core reactor equations. Therefore, the calculation of each coefficient will be described in detail. In all cases the coefficient was determined from the reactivity difference between two static model calculations.

Fuel mass. - The fuel density was varied between two calculations of the same configuration.

Fuel temperature. - Only the effect of a temperature change on the microscopic cross sections of the fuel is considered here. In all calculations the low-energy neutron spectrum was assumed to be determined by the moderator temperature only. Thus, a fuel temperature change was represented by a nucleus temperature change in the calculation of thermal cross sections. The result was a redistribution of the energy transfer cross sections. Uranium-235 was considered to be sufficiently like a 1/v absorber that the nucleus temperature had no effect on absorption cross sections (ref. 17).

Fuel radius. - At a constant total fuel loading in the cavity, the fuel radius was varied. Since propellant volume was necessarily reduced by increasing the fuel radius, the

hydrogen density was varied to preserve the total number of hydrogen atoms in each calculation.

Propellant mass. - At constant fuel loading and density, the propellant mass was varied by changing the hydrogen density in the cavity region.

Propellant temperature. - The same procedure as for the fuel temperature coefficient was used because the low-energy neutron spectrum in the propellant region was also assumed to be determined by the moderator temperature.

Moderator temperature. - Again, only the effect of temperature change on microscopic cross sections was considered. However, a moderator temperature change was assumed to affect the neutron spectrum in all regions of the reactor. The BeO nucleus temperature change was also considered. The effect was to change low-energy absorption and energy transfer cross sections in all reactor regions.

As indicated, a basic assumption of the temperature effects on reactivity coefficients is that the low-energy neutron spectrum in all reactor regions is determined solely by the moderator temperature. Obviously this is not exact because of the upscattering effect observed in the hot hydrogen; but, judging from the fact that the fuel, feed hydrogen, and propellant hydrogen regions are all of the order of 1 or less mean free paths wide, the deviation is probably not large.

Design Perturbations

An interest in a different form of heat exchanger (pebble bed) led to the calculation of reactivity worth of a shell of material located at the inner edge of the reflector in the reference reactor. A 0.625-centimeter- (1/4-in.-) thick shell of separated Mo was worth -19 percent $\Delta k/k$. This can be translated into critical mass increase by the use of fuel coefficients from figure 4 for the reference reactor configuration. For example, the reference critical mass of a 3.058-meter- (10-ft-) diameter, 0.762-meter- (2.5-ft-) thick reflected configuration would increase from 29.2 to 62 kilograms. The corresponding pressure would be 120 MN/m^2 (1185 atm). The critical mass for this configuration as determined from equations (1) and (2) would be well beyond the range studied in this report. Therefore, any design configuration that would require metallic shells located between the reflector-moderator and the reactor cavity was not considered further. Also, this should give some indication of the reactivity penalty of using any structural material other than BeO (or other low-cross-section material such as beryllium or carbon) to construct the cavity liner.

Possible use of tungsten as the propellant seed material because of its high melting point led to calculation of its reactivity effect. For a reference reactor the reactivity change was -0.09 percent $\Delta k/k$ when tungsten was substituted for U^{238} in the propellant

and feed hydrogen regions. Thus it would appear that the nuclear design is insensitive to the seed material since tungsten represents a relatively strong neutron absorber.

CONCLUSIONS

A procedure was developed for determining the critical mass as a function of propellant pressure of a coaxial-flow gas-core reactor for rocket propulsion. Data were generated for a 196 600-newton- (44 200-lbf-) thrust, 4400-second specific impulse engine with a fuel-diameter-to-cavity-diameter ratio of 0.67. Calculations were made for cavity diameters of 3.048, 3.658, and 4.267 meters (10, 12, and 14 ft), reflector thickness from 0.457 to 0.762 meter (1.5 to 2.5 ft), a cavity temperature distribution of 1000 to 27 000 K, and up to 6-volume-percent separated Mo in the reflector for structural purposes. The following additional conclusions were drawn from these calculations:

1. Consideration in the criticality calculations of the propellant pressure required for fuel containment significantly affects the predicted fuel mass in a gas-core reactor.

2. Critical fuel loadings are sufficiently sensitive to parasitic absorption of neutrons that only small amounts (a few percent of the reflector-moderator volume) of separated molybdenum can be used as a structural material. Because of their higher neutron absorption cross sections, other high-temperature structural materials could not be used.

3. Spectrum hardening due to neutron upscattering in high-temperature hydrogen has a significant negative reactivity effect. Reactivity decreased 15 percent $\Delta k/k$ when the hydrogen propellant temperature was increased from 1600 to 10 600 K at constant density.

4. For a fixed set of reactor conditions of thrust, specific impulse, fuel-diameter-to-cavity-diameter ratio, and cavity diameter a limiting pressure (or fuel loading) exists above which a reactor cannot be made critical by increased fuel loading under operating conditions. For the reference conditions this pressure is 73, 69, and 62 MN/m^2 for cavity diameters of 3.048, 3.658, and 4.267 meters, respectively.

Lewis Research Center,
National Aeronautics and Space Administration,
Cleveland, Ohio, February 1, 1972,
112-28.

APPENDIX A

CALCULATIONAL TREATMENT OF HYDROGEN TEMPERATURE DISTRIBUTION

Analytical representation of the hydrogen temperature distribution in the reactor cavity was accomplished by replacing the continuous distribution with five zones (spherical shells). Since temperature was assumed to be the more important variable (as opposed to density), zone boundaries were determined by selecting approximately equal temperature intervals along the linear portion of figure 12 and closer intervals near the cavity liner. Corresponding hydrogen densities were also obtained from figure 12. The average temperature in each zone was obtained by

$$\overline{T} = \frac{\int T(r)\rho(r)r^2\,dr}{\int \rho(r)r^2\,dr}$$

for each zone and the average density by

$$\overline{\rho} = \frac{\int \rho(r)r^2\,dr}{\int r^2\,dr}$$

where the integration limits are the zone radii. These data are itemized in table X. For larger diameter configurations the zone boundaries were scaled by conserving the volume fractions of each region.

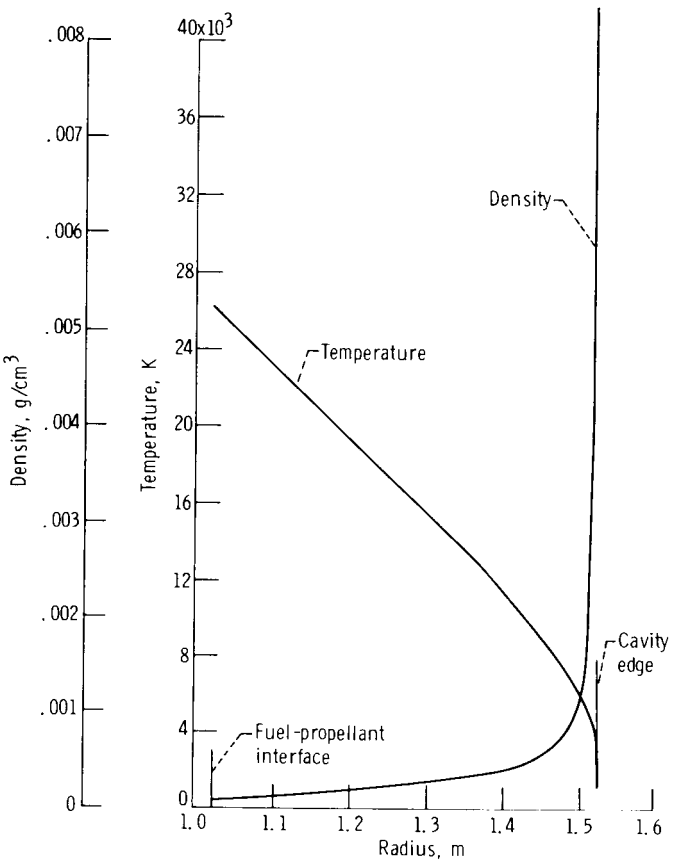

Figure 12. - Hydrogen temperature and density in cavity of gas-core reactor. Cavity diameter, 3.048 meter (10 ft); pressure, 40.5 MN/m^2 (400 atm); thrust, 196 600 newtons (44 200 lbf); specific impulse, 4400 seconds.

TABLE X. - FIVE-ZONE REPRESENTATION

OF CAVITY HYDROGEN DISTRIBUTION

Zone	Average temperature, K	Density, g/cm^3	Boundary, m	
			Inner	Outer
I	22 400	0.000178	1.02	1.19
II	16 200	.000296	1.19	1.35
III	10 200	.000531	1.35	1.47
IV	6 330	.00111	1.47	1.51
V	4 160	.00217	1.51	1.524

APPENDIX B

HYDROGEN DATA

At the temperatures and pressures of interest for a gas core reactor, hydrogen is in various stages of dissociation; and therefore the gas law is invalid for calculating gas density. For this report, densities for reference configuration calculations at 40.5-MN/m^2 (400-atm) pressure are plotted in figure 13. Density variation with pressure at 10 600 K is shown in figure 14. These data were calculated from procedures described in reference 11.

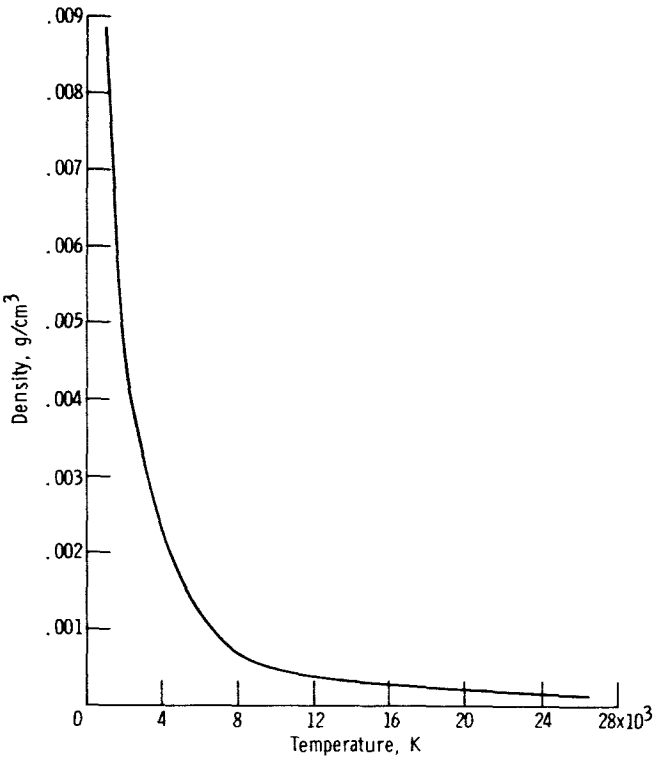

Figure 13. - Hydrogen density at 40.5 MN/m^2 as function of temperature.

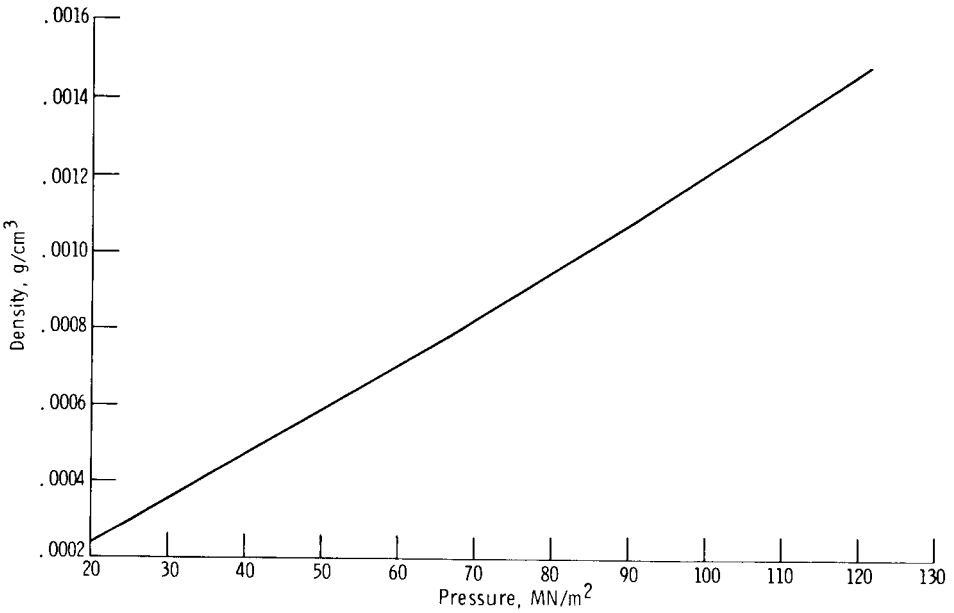

Figure 14. - Hydrogen density at 10 600 K as function of pressure.

REFERENCES

1. Rom, Frank E.: Comments on the Feasibility of Developing Gas-Core Nuclear Reactors. Presented at the Oklahoma State Univ. Frontiers of Power Technology Conference, Stillwater, Okla., Oct. 23-24, 1969.

2. Clement, J. D.; and Williams, J. R.: Gas-Core Reactor Technology. Reactor Tech., vol. 13, no. 3, Summer 1970, pp. 226-251.

3. McLafferty, George H.: Gas Core Nuclear Rockets. Nucl. News, vol. 13, no. 10, Oct. 1970, pp. 48-54.

4. Ragsdale, Robert G.; and Willis, Edward A., Jr.: Gas-Core Rocket Reactors - A New Look. Paper 71-641, AIAA, June 1971.

5. Taylor, Maynard F.; Whitmarsh, Charles W.; Siroky, Paul J., Jr; and Iwanczyk, Louis C.: The Open Cycle Gas-Core Nuclear Rocket Engine - Some Engineering Considerations. 2nd Symposium on Uranium Plasmas: Research and Applications, Atlanta, Ga., Nov. 15-17, 1971.

6. Hyland, Robert E.: Evaluation of Critical Mass for Open-Cycle Gas-Core Rocket Reactors. Nucl. Tech., vol. 12, no. 2, Oct. 1971, pp. 152-161.

7. Ragsdale, Robert G.: Relationship Between Engine Parameters and the Fuel Mass Contained in an Open-Cycle Gas-Core Reactor. Research on Uranium Plasmas and Their Technological Applications. NASA SP-236, 1971, pp. 13-22.

8. Bennett, John C.; and Johnson, Bruce V.: Experimental Study of One- and Two-Component Low-Turbulence Confined Coaxial Flows. NASA CR-1851, 1971.

9. Kunze, J. F.; Lofthouse, J. H.; Suckling, D. H.; and Hyland, R. E.: Flow Mixing, Reactivity Effects in the Gas Core Reactor. Trans. ANS, vol. 14, no. 1, June 1971, p. 11.

10. Anon.: AEC Schedule of Base Charges and Standard Table of Enriching Services. Federal Register, vol. 32, no. 230, 1967.

11. Patch, R. W.: Components of a Hydrogen Plasma Including Minor Species. NASA TN D-4993, 1969.

12. Barber, Clayton E.: A FORTRAN IV Two-Dimensional Discrete Angular Segmentation Transport Program. NASA TN D-3573, 1966.

13. Henderson, W. B.; and Kunze, J. F.: Analysis of Cavity Reactor Experiments. Rep. GEMP-689, General Electric Co. (NASA CR-72484), Jan. 1969.

14. Joanou, G. D.; and Dudek, J. S.: GAM-II. A B_3 Code for the Calculation of Fast-Neutron Spectra and Associated Multigroup Constants. Rep. GA-4265, General Atomic Div., General Dynamics Corp., Sept. 16, 1963.

15. Joanou, G. D.; Smith, C. V.; and Vieweg, H. A.: GATHER II. An IBM-7090 FORTRAN-II Program for the Computation of Thermal-Neutron Spectra and Associated Multigroup Cross Sections. Rep. GA-4132, General Atomics Div., General Dynamics Corp., July 8, 1963.

16. Kunze, J. F.; Pincock, G. D.; and Hyland, R. E.: Cavity Reactor Critical Experiments. Nucl. Appl., vol. 6, no. 2, Feb. 1969, pp. 104-115.

17. Murray, Raymond L.: The Reaction Rate of Neutrons in a Maxwellian Medium. Nucl. Sci. Eng., vol. 26, no. 3, Nov. 1966, pp. 362-365.

18. Lantz, Edward; Mayo, Wendell; Westfall, Robert M.; and Anderson, John L., Jr.: Small High-Temperature Nuclear Reactors for Space Power. NASA TN D-4371, 1968.

NASA-Langley, 1972 — 22 E-6390